Progress In Electromagnetics Research Letters, Vol. 50, 117–123, 2014

A Novel Compact Planar Triple-Band Monopole Antenna for WLAN/WiMAX Applications

Shan Shan Huang[1, 2], Jun Li[1, 3, *], and Jian Zhong Zhao[1]

Abstract—In this article, a novel compact triple-band monopole antenna for WLAN/WiMAX applications is proposed. The proposed antenna is designed on an FR-4 substrate with thickness of 0.8 mm, relative permittivity of 4.4 and loss tangent of 0.02. It consists of a square ring, an open ended stub, and an inverted T-shaped stub. Three bands covering 2.3–2.76, 3.387–3.73, and 4.97–6.28 GHz are achieved, which cover all the 2.5/3.5/5.5 GHz WiMAX and 2.4/5.2/5.8 GHz WLAN operation bands. Moreover, the presented antenna has a compact size of $24 \times 36\,\text{mm}^2$. Experimental results show that the proposed antenna gives good gains and has nearly omnidirectional radiation patterns across all the operation bands.

1. INTRODUCTION

In recent years, wireless local area network (WLAN) and worldwide interoperability for microwave access (WiMAX) have been developed rapidly. Many researchers pay lots of attention to designing antennas with characteristics of multi-band, low-profile, compact size and omnidirectional pattern for multi-band multi-service systems, especially for WLAN and WiMAX applications in wireless communication systems. So, a triple-band antenna is required. Many multi-band antennas [1–15] and ultra-wideband (UWB) antennas [16] have been proposed. In [1], the antenna consists of three "ears" type strips, and three bands can be created by the three "ears". In [2], a reconfigurable antenna is realized by using many open-stubs intersecting with each other. By properly etching an SRR slot on the radiating element of an UWB antenna, two notched bands are achieved in [3]. A coplanar waveguide (CPW)-fed planar antenna with an inverted-L strip, a split-ring slot, and a Y-shaped slot is proposed in [4]. Triple-band CPW-fed antennas with three pairs of inverted-L strips and asymmetric ring are presented in [6, 7], respectively. Dual- and triple-band slot antennas are proposed in [8, 9], and literature [10] reports a modified swastika shape patch antenna. Multi-band monopole antennas have been widely investigated in [11–16]. In [11], a triple-band antenna is formed by inserting an open ended U-shaped slot, two I-shaped notched slots on the patch, and a complex structure of ground. In [12], the presented antenna consists of an S-shaped stub and a square ring on the top layer. A pair of coupled dual-U-shaped radiators is employed to realize triple-band operation in [13]. In [14], a triple-band antenna consists of a horizontal H-shaped patch, an L-shaped open end stub, and a deformed inverted T-shaped stub is proposed. Although these antennas exhibit their own merits, they still need to be improved. For example, the design procedures are complex, and the costs are high in [1, 11, 12]. Omnidirectional radiation patterns cannot be achieved in [2]. The third band of the antenna introduced in [11] cannot cover the WLAN operation band. Only two operating bands are involved in [5, 8], and only three operation bands for WiMAX applications are designed in [13], which limit the numbers of working modes in portable devices. UWB antenna [16] can cover all the operating bands. However, frequency interference cannot be avoided when the UWB antennas are used in WLAN/WiMAX systems.

Received 29 July 2014, Accepted 3 December 2014, Scheduled 19 December 2014

* Corresponding author: Jun Li (lijun_njust@163.com).

[1] Ministerial Key Laboratory of JGMT, Nanjing University of Science and Technology, Nanjing 210094, China. [2] Spreadtrum Communications Inc., Shanghai 201203, China. [3] Huawei Technologies Co., Ltd., Shanghai 200121, China.

In this paper, a novel compact planar triple-band monopole antenna using square ring patch for WLAN/WiMAX applications is presented. It consists of a square ring, an open tuning stub and an inverted T-shaped stub. Three bands covering 2.3–2.75, 3.38–3.7, and 4.91–6.28 GHz are obtained, which cover the 2.5/3.5/5.5 GHz WiMAX and 2.4/5.2/5.8 GHz WLAN bands. The structure of the proposed antenna is much simpler than those presented in [1–12]. Also, this antenna exhibits higher gain than the one proposed in [3]. A prototype antenna is fabricated and measured, and the measurement agrees well with the simulation, which shows the merits of better performance of interference suppression and compact size of $24 \times 36\,\text{mm}^2$.

In Section 2, the configuration and implementation approach of the proposed antenna are discussed. In Section 3, simulated and measured results are presented. The radiation patterns and peak gains of the proposed antenna are given and discussed. Finally, a brief conclusion is provided in Section 4.

2. ANTENNA DESIGN

Figure 1 shows the geometrical configuration of the proposed triple-band monopole antenna with an open tuning stub, square ring and an inverted T-shaped stub. The antenna is designed on an FR-4 substrate with thickness of 0.8 mm, dielectric constant of 4.4 and loss tangent of 0.02. A 50 Ω feedline connected with a 1.5 mm wide microstrip line is used to feed the antenna.

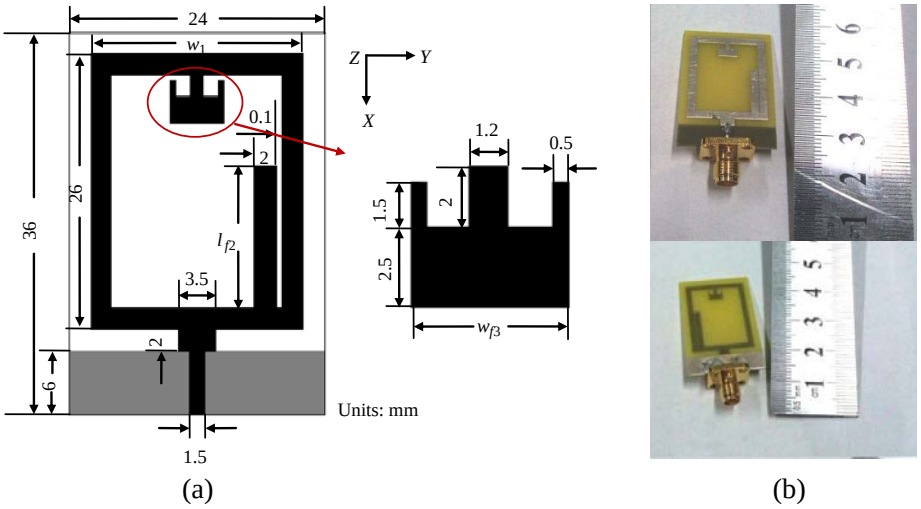

Figure 1. (a) Configuration of the proposed antenna. (b) Photograph of the fabricated prototype antenna.

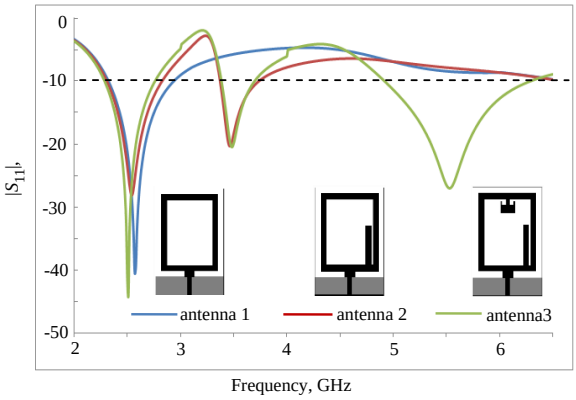

Figure 2. Simulated return losses of involved antennas.

The design procedure is as follows. Firstly, the lower band at about 2.33–2.93 GHz is determined by the square ring (antenna 1 in the inset of Figure 2).

$$f = \frac{c}{\sqrt{\varepsilon_{eff}} \cdot \lambda_g} \tag{1}$$

$$\sqrt{\varepsilon_{eff}} \approx \frac{\varepsilon_r + 1}{2} \tag{2}$$

where c is the speed of light in free space, λ_g the guided wavelength calculated at the desired resonant frequency f, and ε_{eff} the effective dielectric constant. l_{f1} denotes the semi-perimeter of the square ring, i.e., $l_{f1} \approx 26\,\text{mm} + w_1$ in this design, and when l_{f1} equals a half of the guided wavelength at the center frequency of the first band (λ_{g1}), the resonance occurs. So, the center frequency of the first band can be obtained according to Equations (1) and (2) by applying $\lambda_{g1} = 2l_{f1}$.

Secondly, the middle band is achieved by loading an open ended stub to the square ring (as can be seen in antenna 2 in Figure 2), thus, the resonance at about 3.5 GHz is excited. l_{f2} is the length of the open ended stub, and its length is about a quarter of the guided wavelength at the center frequency of the second band (λ_{g2}), namely, $l_{f2} = \lambda_{g2}/4$. Also, the center frequency of the second band can be calculated by using Equations (1) and (2).

Then, the upper band at about 4.91–6.28 GHz is created by the inverted T-shaped stub (as shown in antenna 3 in Figure 2). And the performance of the third band centered at 5.5 GHz can be tuned by adjusting the length of inverted T-shaped stub. At last, by adjusting the position and dimension of the square ring, open ended stub, inverted T-shaped stub and the length and width of matching line, triple-band frequency response centered at about 2.5/3.5/5.5 GHz is achieved.

The simulated return losses ($|S_{11}|$) and specific configurations of these three antennas are illustrated in Figure 2. The simulation works of the proposed antenna are performed by a commercial full-wave electromagnetic (EM) simulator ANSYS HFSS 13.0.

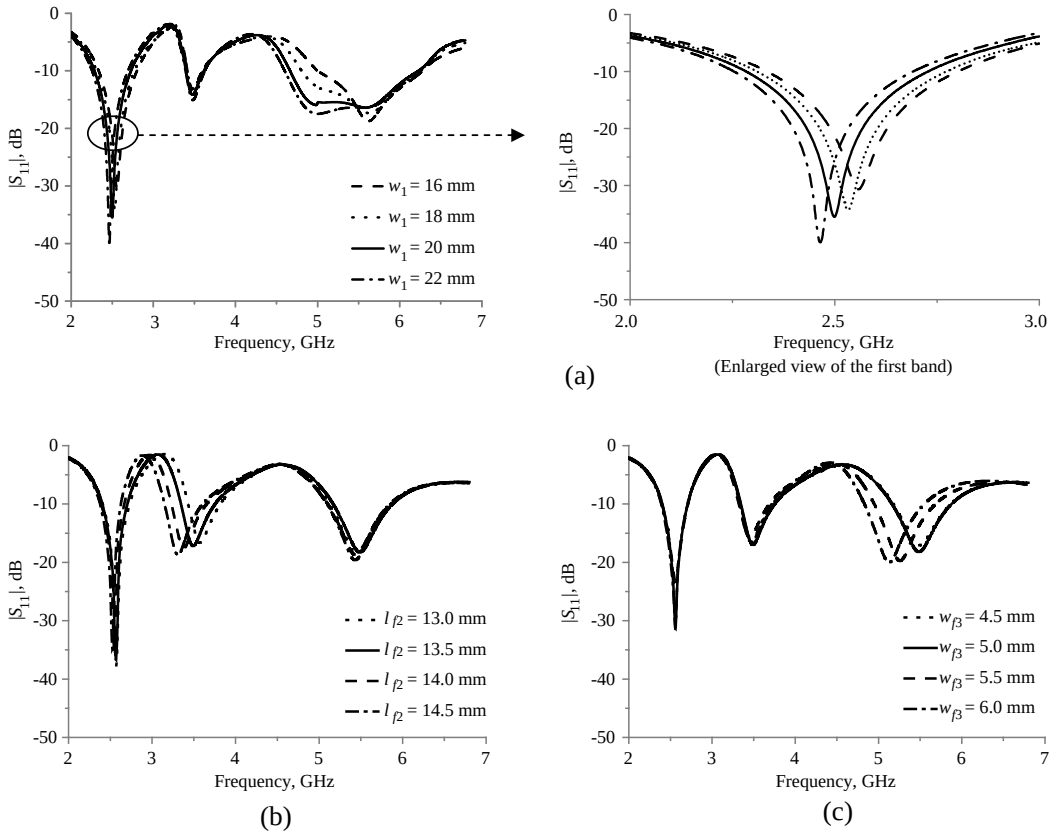

Figure 3. Simulated $|S_{11}|$ of the proposed triple-band antenna with varied (a) w_1, (b) l_{f2}, and (c) w_{f3}.

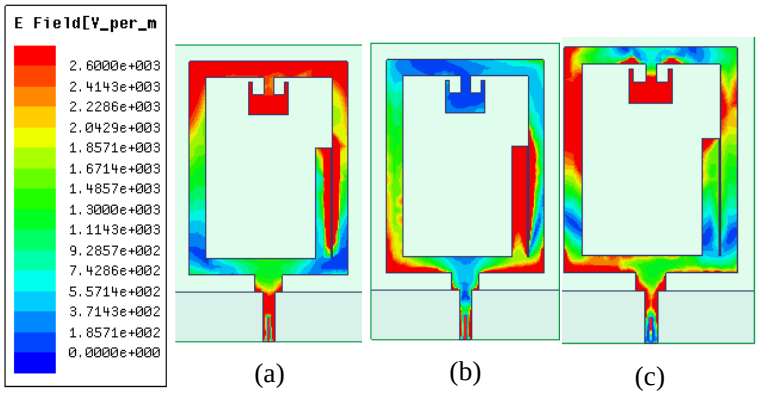

Figure 4. Simulated surface current distributions of the proposed antenna at (a) 2.5 GHz, (b) 3.5 GHz, and (c) 5.5 GHz.

The frequency response of the proposed triple-band antenna is affected by different parameters. Figure 3 illustrates the simulated $|S_{11}|$ curves with varied l_{f2} and w_{f3}. Figure 3(a) depicts the variation of $|S_{11}|$ with varied w_1, and narrowband view of the first band is also plotted. As can be seen from Figure 3(a), center frequency of the first band decreases with the increase of w_1. Moreover, bandwidth of the first band is also influenced by w_1, and it increases when w_1 increases. Figure 3(b) shows the simulated $|S_{11}|$ curves with varied l_{f2}. It is clear that when l_{f2} increases, center frequency of the second band decreases, whereas the first and third ones are almost unchanged. Variation of the $|S_{11}|$ with different w_{f3} is plotted in Figure 3(c). It can be seen from Figure 3(c) that w_{f3} only influences the third band, and center frequency of the third band decreases with the increase of w_{f3}. According to the above analysis, the three bands of the proposed triple-band antenna can be tuned independently by changing the values of w_1, l_{f2}, and w_{f3}, respectively.

In order to further explain the behaviour of the proposed triple-band antenna, the surface current distributions at frequencies of 2.5, 3.5, and 5.5 GHz are plotted in Figure 4. One can clearly observe from Figure 4 that the surface current distributions at these three frequencies are quite different. For the first resonant frequency at about 2.5 GHz, most surface current is distributed on the square ring of antenna 1 as shown in Figure 4(a), and the semi-perimeter of the square ring (l_{f1}) is about a half of the guided wavelength. Thus, the center frequency of the first band is mainly determined by l_{f1}, which is consistent with the above analysis. In addition, the inverted T-shaped stub also has slight effects on the first band as can be seen in Figure 4(a). As indicated in Figure 4(b), the surface current distribution becomes more concentrated on the loaded open ended stub of antenna 2 at about 3.5 GHz. Therefore, center frequency of the second band can be controlled by the length of the open stub. Figure 4(c) plots the surface current distribution of the proposed antenna at the third resonant frequency (5.5 GHz), which reveals that the surface current is more concentrated on antenna 3, and the inverted T-shaped stub can be utilized to control the third band. In summary, the surface current distributions are consistent with the above analysis.

3. RESULTS AND DISCUSSIONS

Based on the above-mentioned design method, a triple-band antenna prototype is designed and fabricated. It is printed on a low-cost FR-4 substrate with a thickness of 0.8 mm, dielectric constant of 4.4, and loss tangent of 0.02. The physical dimensions are labelled in Figure 1(a), where $w_1 = 20$ mm, $l_{f2} = 13.4$ mm, $w_{f3} = 5$ mm. The simulated and measured return losses of the proposed antenna are depicted in Figure 5. Its performance is obtained in an Anechoic Chamber with an Agilent E8362C. As can be observed in Figure 5, the bandwidths of three bands are 460 MHz (2.3–2.76 GHz), 343 MHz (3.387–3.73 GHz), and 1370 MHz (4.97–6.28 GHz), respectively. It is obvious that, it covers the whole WLAN (2.45–2.4835 GHz, 5.16–5.35 GHz, and 5.725–5.85 GHz) and WiMAX (2.5–2.69 GHz, 3.4–3.69 GHz, and 5.28–5.85 GHz) operation bands. Moreover, good band-to-band isolation and low

in-band return loss are obtained. Good agreement between the simulated and measured results are observed from Figure 5. There exist some discrepancies at the first band, which may be due to the fabrication tolerance and the difference between the simulated and measured environment.

Figures 6(a), (b), and (c) are the simulated and measured far-field radiation patterns in xz-plane (E-plane) and yz-plane (H-plane) of the proposed antenna at 2.5, 3.5, and 5.5 GHz, respectively. Figure 6 indicates that the radiation in E-plane is always bidirectional radiation, and the radiation in H-plane

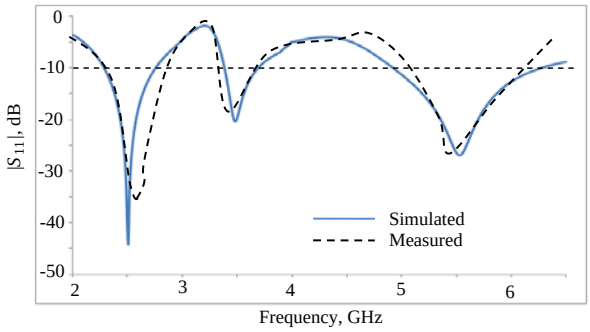

Figure 5. Simulated and measured return losses of the proposed antenna.

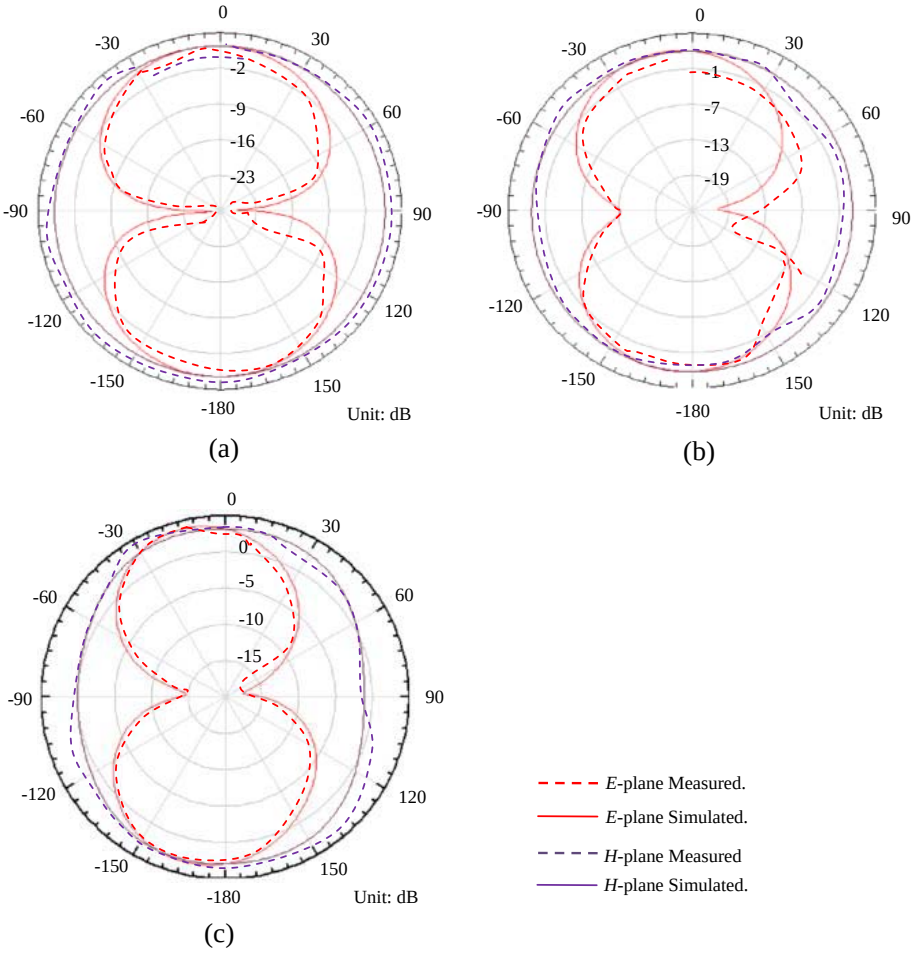

Figure 6. Simulated and measured radiation patterns of the proposed antenna at (a) 2.5 GHz, (b) 3.5 GHz, and (c) 5.5 GHz.

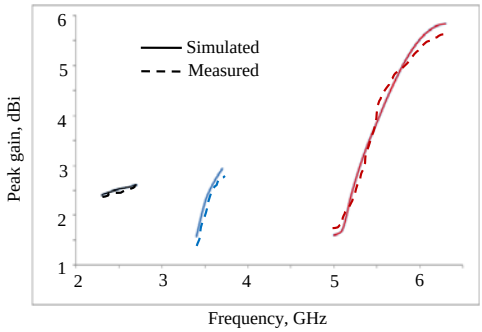

Figure 7. Simulated and measured peak gain of the proposed antenna.

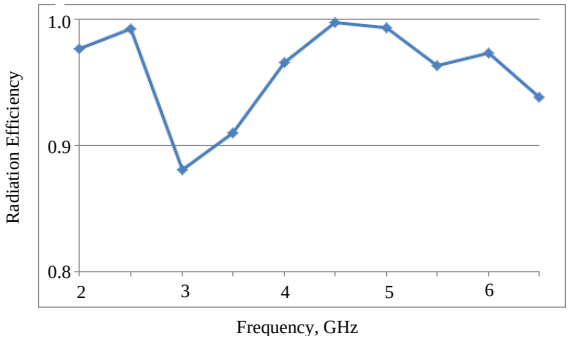

Figure 8. Radiation efficiency of the proposed antenna.

is always omnidirectional and has stable radiation. The simulated and measured peak gain patterns of the three bands are depicted in Figure 7. As can be seen from Figure 7 that the average peak gains of the three bands are 2.52, 2.37, and 4.15 dBi for 2.5, 3.5, and 5.5 GHz bands, respectively. Figure 8 plots the radiation efficiency of the proposed antenna. It can be observed that the radiation efficiency is better than 85% across all the operation bands. All these merits reveal that the proposed triple-band antenna is very suitable for modern WLAN/WiMAX wireless communication systems.

4. CONCLUSION

In this paper, a novel compact triple-band monopole antenna for WLAN/WiMAX applications is proposed. It consists of a square ring as the primary radiation element, an open ended stub loaded on one side of square ring and an inverted T-shaped stub loaded on the other side. By using three different types of resonant structure, the proposed antenna can earn good triple-band performance which effectively covers all the WLAN/WiMAX operation bands. A triple-band prototype antenna is then designed, implemented, and measured. The measured results show good agreement with the simulated ones. Owing to the characteristics of compact size, omnidirectional radiation pattern and stable gain of the proposed antenna, it is more applicable in modern WLAN/WiMAX wireless communication systems.

REFERENCES

1. Zhai, H.-Q., et al., "A compact printed antenna for triple-band WLAN/WiMAX applications," *IEEE Antennas and Wireless Propagation Letters*, Vol. 12, 65–68, 2013.
2. Ressiguier, D., J. Costantine, Y. Tawk, and C.-G. Christodoulou, "A reconfigurable multi-band microstrip antenna based on open ended microstrip lines," *3rd European Conference on Antennas and Propagation, EuCAP 2009*, 792–795, 2009.
3. Cai, L.-Y., G. Zeng, H.-C. Yang, and Y.-Z. Cai, "Integrated bluetooth and multi-band ultra-wideband antenna," *Electron. Lett.*, Vol. 47, No. 12, 688–689, 2011.
4. Liu, P., Y. Zou, B. Xie, X. Liu, and B. Sun, "Compact CPW-fed tri-band printed antenna with meandering split-ring slot for WLAN/WiMAX applications," *IEEE Antennas and Wireless Propagation Letters*, Vol. 11, 1242–1244, 2012.
5. Lizzi, L., F. Viani, and A. Massa, "Dual-band spline-shaped PCB antenna for Wi-Fi applications," *IEEE Antennas and Wireless Propagation Letters*, Vol. 8, 616–619, 2009.
6. Huang, S. S., J. Li, and J. Z. Zhao, "Compact CPW-fed tri-band antenna for WLAN/WiMAX applications," *Progress In Electromagnetics Research C*, Vol. 49, 39–45, 2014.
7. Huang, S. S., J. Li, and J. Z. Zhao, "Miniaturized CPW-fed triband antenna with asymmetric ring for WLAN/WiMAX applications," *Journal of Computer Networks and Communications*, Vol. 2014, Article ID 419642, 8 Pages, 2014.

8. Ojaroudi, N. and N. Ghadimi, "Dual-band CPW-fed slot antenna for LTE and WiBro applications," *Microw. Opt. Technol. Lett.*, Vol. 56, No. 5, 1013–1015, May 2014.
9. Zhao, Q., S.-X. Gong, W. Jiang, B. Yang, and J. Xie, "Compact wide-slot tri-band antenna for WLAN/WiMAX applications," *Progress In Electromagnetics Research Letters*, Vol. 18, 9–18, 2010.
10. Samsuzzaman, M., et al., "Compact modified swastika shape patch antenna for WLAN/WiMAX applications," *International Journal of Antennas and Propagation*, Vol. 2014, Article ID 825697, 8 Pages, 2014.
11. Wang, P., et al., "Compact CPW-fed planar monopole antenna with distinct triple bands for WiFi/WiMAX applications," *Electron. Lett.*, Vol. 48, No. 7, 357–359, 2012.
12. Xu, Y., Y.-C. Jiao, and Y.-C. Luan, "Compact CPW-fed printed mono-pole antenna with triple-band characteristics for WLAN/WiMAX applications," *Electron. Lett.*, Vol. 48, No. 24, 1519–1520, 2012.
13. Koo, T. W., et al., "A coupled dual-U-shaped monopole antenna for WiMAX triple-band operation," *Microw. Opt. Technol. Lett.*, Vol. 53, No. 4, 745–748, Apr. 2011.
14. Huang, S. S., J. Li, and J. Z. Zhao, "Design of a compact triple-band monopole planar antenna for WLAN/WiMAX applications," *Progress In Electromagnetics Research C*, Vol. 48, 29–35, 2014.
15. Li, J., S. S. Huang, and J. Z. Zhao, "A compact CPW-fed tri-band antenna for WLAN/WiMAX applications," *Open Science Journal of Electrical and Electronic Engineering*, Vol. 1, No. 4, 21–25, 2014.
16. Thwin, S. S., "Compact asymmetric inverted cone ring monopole antenna for UWB applications," *Progress In Electromagnetics Research Letters*, Vol. 36, 57–65, 2013.